Composites Part B 165 (2019) 65–74

Contents lists available at ScienceDirect

Composites Part B

journal homepage: www.elsevier.com/locate/compositesb

A comparative study on effects of natural and synthesised nano-clays on the fire and mechanical properties of epoxy composites

M. Rajaei*, N.K. Kim, S. Bickerton, D. Bhattacharyya

Centre for Advanced Composite Materials, Department of Mechanical Engineering, The University of Auckland, Auckland, New Zealand

ARTICLE INFO

Keywords:
Thermosetting resin
Nano-structures
Thermal properties
Mechanical properties

ABSTRACT

In this research, two nano-clays, halloysite nano-tube (HNT) and layered double hydroxide (LDH), were employed to compare fire and mechanical properties of epoxy composites based on ammonium polyphosphate (APP) and each of the two nano-clays. The results showed that the combination of APP and nano-clay achieved a significant reduction (approx. 87%) in peak heat release rate of epoxy resin. The comparative analysis also demonstrated that the total heat release of the composite including HNT was approx. 18% lower than that of the LDH based composite. Moreover, HNT generated higher tensile properties in the composite. Overall, the HNT (~1.5 USD/kg) is a more cost-effective nano-clay than LDH (~180 USD/kg) to effectively improve the fire resistance and maintain the mechanical properties of epoxy composites.

1. Introduction

Nano-clays are one of the most widely used nano-particles in the field of polymer composites, since they have the potential to enhance the flame retardance, thermal, mechanical and gas barrier properties of polymers [1–3]. There are different types of nano-clays, such as layered double hydroxide (LDH), halloysite nano-tube (HNT), montmorillonite (MMT) and kaolinite. Among them, LDH (commonly named anionic clay) is a relatively new class of anionic lamellar (two dimensional) nano-material comprised of positively charged brucite-like layers with an interlayer region containing charge compensating anions and molecules of solvation, Fig. 1 (a). The general molecular formula of LDH is $[M_{1-x}^{2+}M_x^{3+}(OH)_2]^{x+}A_{x/n}^{n-}.zH_2O$, where M^{2+} and M^{3+} are divalent and trivalent metal cations, such as Mg^{2+} and Al^{3+}, respectively, and A^{n-} is an intercalated organic or inorganic anion, such as CO_3^{2-} and NO_3^- [4]. The cations and intercalated anion can be varied and this can provide tuneable properties for the LDH to be used for different applications, namely thermal stabiliser, flame retardance and scavengers for pollutants [5–7]. The bio-compatibility of the LDH nano-particles also makes them suitable for medical applications [8]. The LDH nano-clay can be formed synthetically and the Mg-Al-LDH is the most frequently used LDH clay [3]. Compared to LDH, HNT is a more abundant and cost-effective natural nano-filler, which has versatile thermal and mechanical properties and a wide range of optical, electrical and energy storage applications [9–11]. HNT is a 1:1 aluminosilicate clay mineral with the chemical formula of $Al_2Si_2O_5(OH)_4$ and hollow tubular structure (one dimensional), Fig. 1 (b), which can be formed as a result of hydrothermal or weathering processes [10,12,13]. In the HNT structure, the water molecules are present between the sheets of SiO_4 and AlO_6 [14].

The effects of both LDH and HNT particles on the thermal and fire-related properties of different polymers have been extensively reported in the literature [4,12,15–17]. It has been generally found that the nano-additives can enhance the thermal stability and flame retardancy of polymers through four different mechanisms: (a) endothermic thermal decomposition (heat sink), (b) formation of a protective char layer on the surface of polymer during the heat and fire exposure, (c) catalysing and reinforcing the char formation and (d) increasing the viscosity of the polymer melt [18]. The layered nano-clays, such as LDH and MMT, can reduce the flammability of polymer nano-composites by migrating the particles toward the surface of the polymer and forming a char (barrier) against heat and volatiles [1,19], whereas the fibrous nano-additives, namely carbon nanotube and HNT, show high thermal stability, thereby facilitating the char formation [1,20]. It has been identified that the presence of nano-particles in the polymer matrices can mainly reduce the heat release rate (HRR) but other important flammability parameters, such as UL-94 rating and limiting oxygen index (LOI), have not been influenced. Therefore, the applications of hybrid flame retardants and nano-particles have been strongly recommended to enhance overall fire performance of polymers, covering different testing conditions [21–23]. Among all flame retardant additives, it has been shown that the combination of intumescent

* Corresponding author.
E-mail address: mraj585@aucklanduni.ac.nz (M. Rajaei).

https://doi.org/10.1016/j.compositesb.2018.11.089
Received 7 July 2018; Received in revised form 4 September 2018; Accepted 22 November 2018
Available online 27 November 2018
1359-8368/

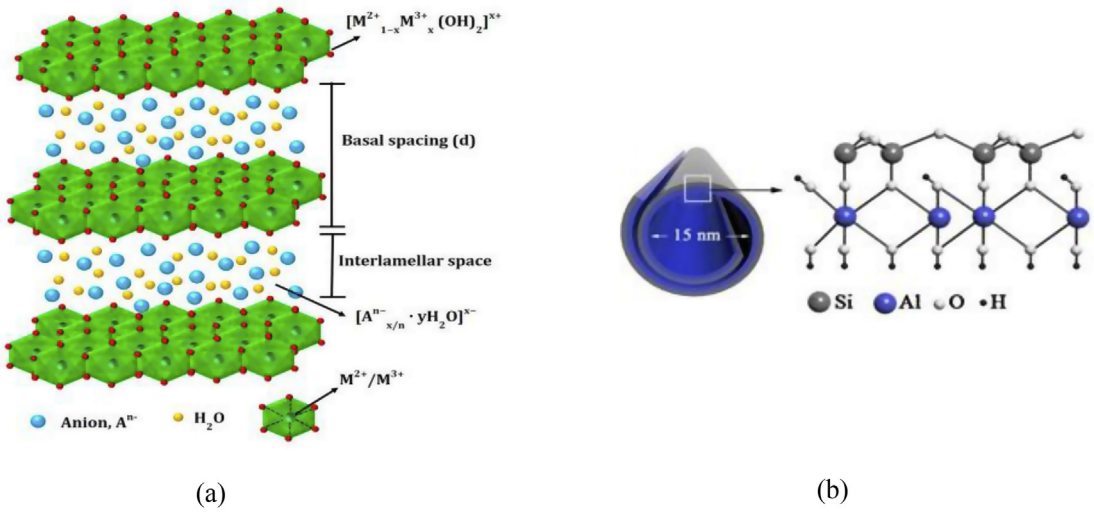

Fig. 1. Schematic illustrations of (a) LDH and (b) HNT [8,13] (Reproduction with permission from Elsevier).

additives and mineral nano-particles provide the suitable flame retardant level for thermoplastic polymers to meet the regulatory standards [22,24–31]. The flame retardancy mechanism of the hybrid additive system has been explained by an effective intumescent char formation on the surface of the polymer, which can act as a physical barrier and protect the underlying material from the heat and flame [32]. The contribution of the nano-particles in this process is to improve the insulating effect of the char [33].

To the best of our knowledge, the combined effects of intumescent flame retardants and nano-clays on fire and mechanical performance of the epoxy based composites have not been comprehensively explored. Furthermore, little has been reported on the comparison between the effects of the LDH and HNT on the flammability of epoxy nano-composites. Therefore, the present paper focuses on characterising and comparing the fire properties of epoxy resin in the presence of LDH and HNT nano-particles. In addition, the combined effects of intumescent APP and the chosen nano-particles on the flame retardancy and mechanical properties of epoxy resin and epoxy/glass fibre composites were investigated. The cone calorimeter, UL-94 vertical burn, and LOI tests were carried out to investigate the flammability of the prepared composites, while tensile, flexural and compression tests were performed to evaluate the mechanical properties.

2. Experimental details

2.1. Materials

Diglycidyl ether of bisphenol A epoxy resin (105 West System epoxy) and polyamine curing agent (206 slow hardener) were obtained from Adhesive Technologies Ltd. (New Zealand). HNT was supplied by Imerys Tableware (New Zealand) and silane, N-(b-aminoethyl)-c-aminopropyltrimethoxysilane, from Sigma Aldrich (New Zealand) was used for the surface treatment of HNT. The stearate intercalated Mg-AL-LDH, $[Mg_2Al(OH)_6](C_{18}H_{35}O_2).3H_2O$, was purchased from Prolabin & Tefarm (Italy). Furthermore, the melamine coated APP (FR CROS 40, Budenheim, Germany) was selected as an intumescent flame retardant. Woven E-glass fabric (2 × 2 twill weave, 300 g/m^2 areal density) was provided by Colan (Australia).

2.2. Sample preparation

2.2.1. Silane modification of HNT

The silane solution was selected to modify the surface of as received HNT and improve the interfacial adhesion of the nano-tubes with the resin. Firstly, 12.36 ml of acetic acid was dissolved into 600 ml of water to obtain 4.5 pH. Then, silane (8.2 ml) was added to the prepared aqueous solution after mixing with 261.6 ml of methanol. The solution was stirred at 60 °C using a ceramic magnetic bar and then 60 g of HNT was added and mixed for 5 h. The silane treated HNT (mHNT) was ground to obtain the powder form after drying in a freeze dryer (Labconco, US) [34].

2.2.2. Epoxy nano-clay blends

The LDH, mHNT and APP particles were dried in an oven at 80 °C for 10 h prior to mixing with epoxy to remove contained moisture content. A three roll mill machine (Torrey Hills Technologies, US) was employed to mix the additives with the resin. The two gaps between the rollers were both adjusted to 20 μm and the mixture was then passed through each gap three times. The hardener was added to the mixture of resin and additives (weight ratio of the resin to hardener was 5.36:1) and stirred rapidly; then the mixture was degassed using a vacuum chamber at room temperature (21 °C) to remove the air bubbles. Finally, the epoxy resin containing additives and hardener was poured into the silicone moulds having standard sample size cavities for fire and mechanical tests and cured at room temperature for 72 h.

2.2.3. Fibre reinforced epoxy composites

The fibre reinforced epoxy composites were prepared by the resin impregnation of the glass fibre plies (8 layers) using the hand lay-up technique, followed by stacking and pressing at 0.7 MPa for 72 h at room temperature. The resultant laminates, which had an average thickness of 2.7 mm and 35 ± 2% fibre volume fraction, were cut into the standard dimensions for the various tests. The reference epoxy/glass fibre composites were also prepared using the same method. Table 1 indicates the composition of samples generated for this research.

2.3. Chemical, thermal and morphological characterisation

Fourier Transform Infrared (FTIR) spectra of HNT, mHNT and LDH were recorded between 4000 and 500 cm^{-1} using a Nicolet FTIR iS 50 spectrometer (Thermo Fisher Scientific, US). In the spectrum of each nano-particle, the energy absorption peaks corresponding to vibration of different atoms or molecules were analysed. Moreover, thermogravimetric analysis (TGA) was carried out to characterise the thermal properties of the epoxy blend and composite samples using a TGA Q5000 instrument (TA Instruments, US). 3–5 mg of sample was placed in an open platinum pan and heated from room temperature to 800 °C at a constant heating rate of 10 °C/min in nitrogen atmosphere.

Table 1
Composition of manufactured epoxy blend and composite samples.

Sample	Epoxy resin/ Hardener (wt%)	LDH (wt%)	mHNT (wt%)	APP (wt%)	Woven Glass Fibre (wt%)
EP	100	0	0	0	0
EP2HNT	98	0	2	0	0
EP2LDH	98	2	0	0	0
EP4LDH	96	4	0	0	0
EP6LDH	94	6	0	0	0
EP18A2LDH	80	2	0	18	0
EP18A2HNT	80	0	2	18	0
EP20A	80	0	0	20	0
EPWF	46.43	0	0	0	53.57
EPWFAHNT	38.44	0	0.96	8.65	51.95
EPWFALDH	38.20	0.96	0	8.59	52.25
EPWFA	38.37	0	0	9.59	52.04

Furthermore, the morphology of the residue after cone calorimeter experiments and the tensile fractured cross-sections of composites were analysed using an environmental scanning electron microscope (ESEM, FEI Quanta 200F, US). A transmission electron microscope (TEM, Tecnai 12, Thermo Fisher Scientific, US) was also employed to observe the nano-particles dispersion in the epoxy matrix.

2.4. Fire testing

The cone calorimeter is a versatile experimental device used to characterise the fire reaction properties of polymers, and other materials. In this study, the dual cone calorimeter (Fire Testing Technology, East Grinstead, UK) was used to evaluate the fire performance of the manufactured samples according to ASTM D1354. Square samples (100 × 100 × 2.7 mm) were preconditioned in a chamber at 23 °C and 50% humidity for at least 48 h before being exposed to a 50 kW/m^2 heat flux in horizontal position by an external cone heater. The reported data are the average of three replicated tests.

UL-94 vertical burn tests were conducted to measure the flame resistance of the blends and composite samples according to ASTM D3801. The flammability of the vertically placed rectangular samples (125 × 13 × 2.7 mm) was measured by two 10 s flame applications on their bottom edges. The samples were classified as V-0 (flame extinguishment within 10 s without dripping), V-1 (flame extinguishment within 30 s without dripping), V-2 (flame extinguishment within 30 s with dripping) ratings or NR (no rating) based on the dripping behaviour, after flame and afterglow times.

Limiting oxygen index (LOI) experiments were carried out according to ASTM D2863 to determine the minimum oxygen concentration, which supports the flaming combustion of the blends and composite samples. Strip samples (130 × 6.5 mm) with thicknesses of 2.7 mm (fibre reinforced composites) and 3 mm (epoxy blends) were tested using an oxygen index meter (Fire Testing Technology, East Grinstead, UK).

2.5. Mechanical testing

Tensile properties of the epoxy nano-clay blends (dumbbell-shaped samples of 3.2 mm thickness, 13 mm width in the narrow section and with overall length of 174 mm) were measured using an Instron universal testing machine (4465). According to ASTM D638, the cross-head speed and the gauge length were 5 mm/min and 50 mm, respectively. The chord tensile moduli were measured between 0.05 and 0.25% strains using a mechanical extensometer. The tensile tests of the fibre reinforced composites (250 mm × 25 mm × 2.7 mm) were carried out at 2 mm/min cross-head speed and 50 mm gauge length based on ASTM D3039. A 100 kN load cell was used and the chord tensile moduli of the reinforced composites were calculated between 0.1 and 0.3% strains.

Flexural properties of the epoxy nano-clay blends and fibre reinforced composites were measured in the three-point bending mode according to ASTM D790 (procedure A). The rectangular samples (60 × 12.7 × 2.7 mm) were tested at a cross-head speed of 1.1 mm/min and 42.2 mm supporting span length.

The compressive strengths of the manufactured fibre reinforced composites were determined by compression tests according to ASTM D6641 (procedure A). The samples (140 × 12 × 2.7 mm) were tested at a fixed 13 mm gauge length and 1.3 mm/min cross-head speed. In all mechanical tests, five tests for each sample type were carried out and the average values were reported.

3. Results and discussion

3.1. FTIR characterisation of nano-particles

Fig. 2 presents the FTIR spectra of HNT, mHNT and LDH particles. It

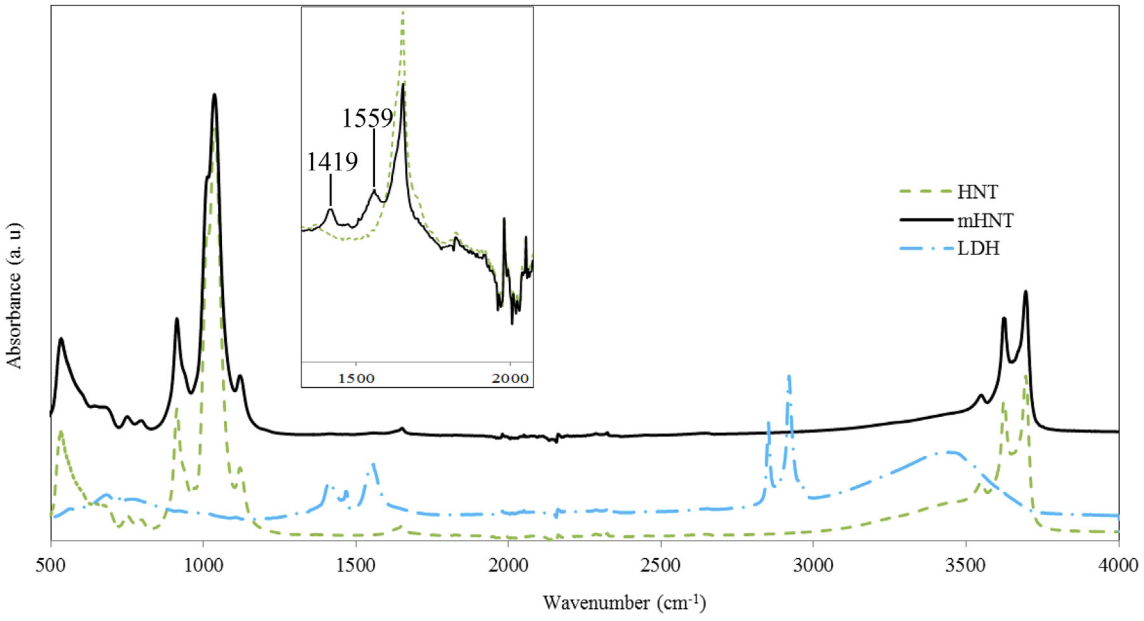

Fig. 2. FTIR spectra of HNT, mHNT and LDH.

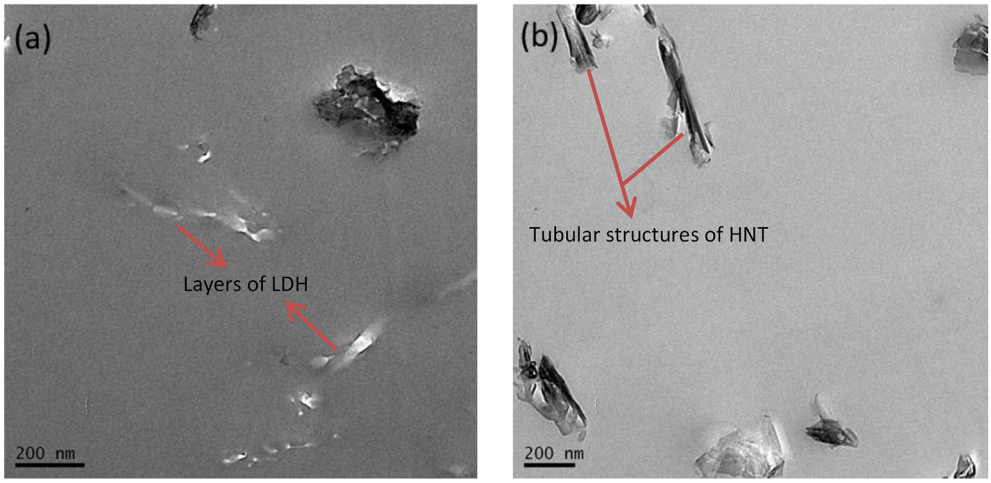

Fig. 3. TEM images of (a) EP2LDH and (b) EP2HNT samples.

is clear that the positions of most bands remained unchanged after modification of HNT, suggesting that the silane treatment did not alter its basic structure. However, the existence of new weak peaks at 1419 and 1559 cm^{-1} in the spectrum of mHNT can be attributed to the vibration of C—N and N—H bands of the silane, respectively [35]. These results may indicate that silane has been successfully grafted on the surface of HNT. Regarding the spectrum of LDH, the absorption peaks at 2800-3000 cm^{-1} can be assigned to the vibration of C—H bands due to the presence of C— H_2 and C— H_3 groups of intercalated stearate anions [36].

3.2. Morphological analysis of epoxy nano-clay blends

Fig. 3(a) and (b) show the TEM images of the EP2LDH and EP2HNT samples, respectively. It can be seen that both LDH and HNT particles were dispersed in the polymer matrix, in spite of formation of some agglomerations. In case of the sample containing LDH, it is discernible that the epoxy chains could penetrate into the LDH galleries to disperse the layers in the matrix, Fig. 3 (a). For the HNT blend, as shown in Fig. 3 (b), the tubular structures of the HNT particles are also observed in the epoxy matrix.

3.3. Fire properties

3.3.1. Epoxy nano-clay blends

Fig. 4 shows the HRR curves of the epoxy resin and nano-clay blends, while Table 2 summarises the cone calorimeter parameters with the UL-94 and LOI tests results. As expected, epoxy resin completely burnt out with a sharp peak heat release rate (PHRR) of 1910 kW/m^2. The addition of 2 wt% HNT to epoxy slightly reduced the PHRR (approximately 17%), while the incorporation of the same loading level of LDH significantly decreased the PHRR (around 58%) of the epoxy resin. The reduction in PHRR for the EP2HNT sample can be explained by the heat sink effect, which is the endothermic de-hydroxylation (at 400–550 °C) of the nano-tubes during the temperature rise. The EP2HNT sample released water, cooling down the heat zone during the thermal decomposition, thereby diluting the fuel and volatiles. The effects of a heat sink and fuel dilution by HNT on the flammability reduction of thermoplastic polymer composites have also been reported in the literature [37,38]. However, the heat sink effect showed limited efficacy to reduce the HRR of the resin compared to those of the well-established condensed phase flame retardant mechanisms.

The EP2LDH (2 wt% LDH) sample also demonstrates the positive effect of LDH on the decrease in PHRR. Compared to the EP2HNT, the significantly lower PHRR was obtained as the LDH can form a ceramic-like char on the surface of the sample. During exposure to heat, the LDH

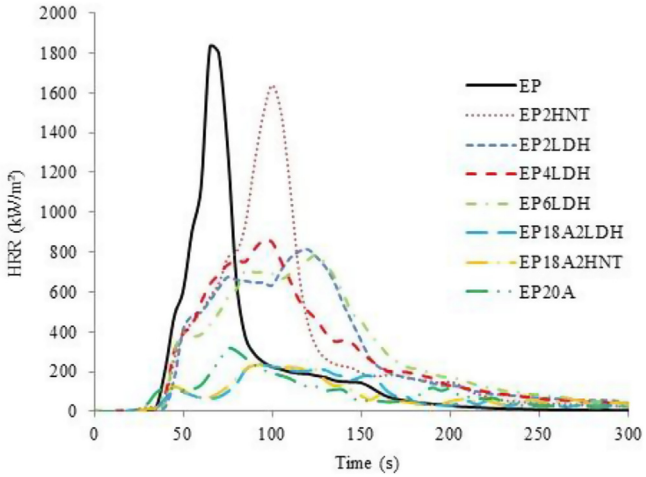

Fig. 4. Heat release rate curves versus time of epoxy resin and blends at 50 kW/m^2 external heat flux.

nano-particles can migrate to the sample surface and yield a char layer (physical barrier), which can protect the underlying material from the heat and flame, thus limiting the combustion. Fig. 5(a) and (b) present the side views of the EP2LDH and EP2HNT samples, respectively, at the end of the tests. It can be clearly observed that the blend in the presence of LDH nano-particles produced a large intumescent char layer, whereas the sample including HNT completely burnt out. On the other hand, the cone calorimeter tests of the epoxy containing 4 and 6 wt% LDH have indicated that the increase in the LDH content does not affect the PHRRs. At the higher loading levels, the agglomerations of the LDH nano-particles may limit the migration of the particles to the surface of the sample to form the char layer. In addition, as shown in Table 2, the total heat release (THR) values of the neat epoxy resin were similar with those of the blends. This behaviour was also observed for nano-composites in previous studies [39,40] and can be explained by the slow but prolonged combustion of the resin in the presence of nano-additives.

On the other hand, the UL-94 and LOI test results in Table 2 show the trivial effects of nano-clays on the flammability of the epoxy blends. In particular, every sample could not achieve any vertical burn rating in spite of the reduction in HRR. This can be explained by the fact that the aforementioned flame retardant mechanism of LDH cannot be applied to provide the self-extinguishing behaviour for the blends when they are directly exposed to a flame. Furthermore, the slight decrease in the LOI value of epoxy resin is observed with the incorporation of the nano-

Table 2
Cone calorimeter parameters, UL-94 and LOI results of epoxy resin and blends.

Sample	Time to ignition (s)	Peak heat release rate (kW/m^2)	Total heat release (MJ/m^2)	UL-94 Rating	Limiting oxygen index (%)
EP	21 ± 1	1910 ± 185	84.4 ± 1.7	No Rating	22.1 ± 0.2
EP2HNT	20 ± 2	1591 ± 68	90.7 ± 1.5	No Rating	19.5 ± 0.2
EP2LDH	21 ± 1	803.4 ± 27.7	87.5 ± 4.6	No Rating	21.6 ± 0.2
EP4LDH	22 ± 2	861.1 ± 8.6	85.4 ± 3.8	No Rating	20. 6 ± 0.2
EP6LDH	20 ± 1	791 ± 33.6	82.9 ± 3.5	No Rating	19.7 ± 0.3
EP18A2LDH	20 ± 2	239.7 ± 12.2	30.3 ± 3.5	V-0	33.2 ± 0.2
EP18A2HNT	20 ± 3	245.5 ± 10.7	26.2 ± 1.8	V-0	32.7 ± 0.2
EP20A	22 ± 2	312.6 ± 12.7	30.8 ± 1.2	V-0	32.6 ± 0.3

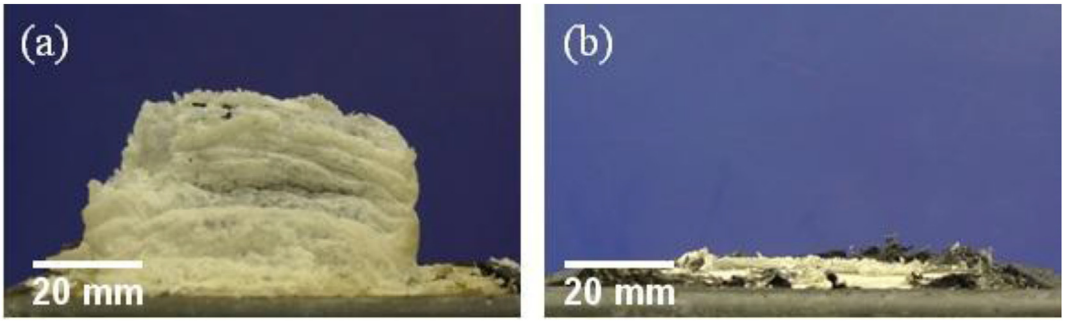

Fig. 5. Side views of (a) EP2LDH and (b) EP2HNT blends after cone calorimeter tests.

particles. The introduction of the nano-clays can increase the viscosity of the polymer during the decomposition process and fix more combustible material (i.e. epoxy resin) in the pyrolysis zone, which consequently can expedite the combustion of the sample and reduce the LOI value [41,42].

According to the results of the UL-94 and LOI tests, it is necessary to enhance the flame retardancy of the epoxy nano-clay blends. In this work, the intumescent APP was used to improve the fire properties of the epoxy blends and the total loading level of the additives (APP and nano-clays) was fixed to 20 wt%, since previous researches showed that this concentration could provide suitable fire properties for epoxy composites [43,44]. Fig. 4 shows that an addition of 18 wt% APP to the EP2LDH and EP2HNT samples resulted in approximately 70 and 84% reductions, respectively, in the PHRRs of the blends. This significant reduction of the flammability can be attributed to the intumescent char formation by APP [43,45,46]. Moreover, the EP18A2LDH and EP18A2HNT samples showed the similar trend of HRR curves with the PHRR values. This can be due to the dominant effect of APP to improve the flame retardant properties of the blends. The role of nano-particles, such as LDH and HNT, in the samples containing APP is to enhance the barrier effect of the intumescent char against the heat and flame [29,33]. The results also demonstrate that the PHRR of the EP18A2LDH and EP18A2HNT samples containing nano-particles are lower compared to that of the epoxy blend filled only with APP, most likely due to the more effective char formation in the presence of both APP and nano-clays. Fig. 6(a) and (b) and (c) present the scanning electron micrographs of the char (outer surface) obtained from the EP20A, EP18A2HNT and EP18A2LDH samples, respectively, after the cone calorimeter tests. Comparing the morphologies of the char demonstrates that the char obtained from the EP18A2HNT has a more compact structure compared to those of the EP20A and EP18A2LDH samples and hence, more effectively limits the heat and oxygen transfer to the underlying material. The total heat released by the EP18A2HNT sample was also lower than those of the EP18A2LDH and EP20A (Table 2), because of the higher efficacy of the char to restrict the combustion process. On the other hand, the char of the EP18A2LDH exhibited an irregular surface with micron sized holes. Even though the EP18A2LDH sample created such a porous char structure during combustion, the significant decrease in the PHRR was observed as the release of H_2O and CO_2 gases from the decomposition of LDH can promote the intumescent behaviour of the char and also dilute the oxygen concentration. In addition, both EP18A2HNT and EP18A2LDH samples achieved a V-0 rating and showed noticeable improvement in the LOI due to the combined effects of APP and nano-clays on the char formation. In particular, the established gas-phase and condensed-phase flame retardant behaviour of LDH and APP, respectively, played an important role in obtaining a slightly lower PHRR and higher LOI of the EP18A2LDH than those of the EP18A2HNT.

3.3.2. Fibre reinforced epoxy composites

Fig. 7 illustrates the HRR curves of the fibre reinforced composites and Table 3 demonstrates the results of the cone calorimeter, U-94 and LOI tests. In general, the fibre reinforced composites released significantly lower heat as compared to those of the blends, obviously due to the decreasing flammable epoxy content. In addition, glass fibres absorb a significant amount heat, since they do not melt or degrade under the radiant heat up to approximately 750 °C [47]. The observed fluctuations in the HRR of the reference epoxy/glass fibre composite during the test can be related to the layered structure of the composite. Similar to the epoxy blends, the incorporation of APP decreased the PHRR of the reference composite (from 453.5 kW/m^2) by approximately 36% as a result of the intumescent char formation. However, a second peak appeared at around 200 kW/m^2 for the EPWFA composite, which might be attributed to the breakage of the char and the thermal feedback from back surface of the sample. It is also noteworthy that the intumescent behaviour of the char decreased in the presence of the glass fibre plies as they maintained their layered structure during the radiant heat exposure. Moreover, further reductions in the first and second PHRRs of the EPWFA composite were observed with the addition of nano-particles. The reason for the decrease in the HRR of the composite was the improvement of the shielding effect of the char surface layer by the nano-particles. Similar PHRR values were recorded from the composites containing LDH and HNT, even though the second peak was lower for the composite including HNT, due to the more compact structure of the char in the presence of HNT, Fig. 6 (b), and its higher resistance against the external heat flux. As the result of the lower second peak of HRR, the THR value of the EPWFAHNT sample was also lower compared to that of the EPWFALDH. Furthermore, the

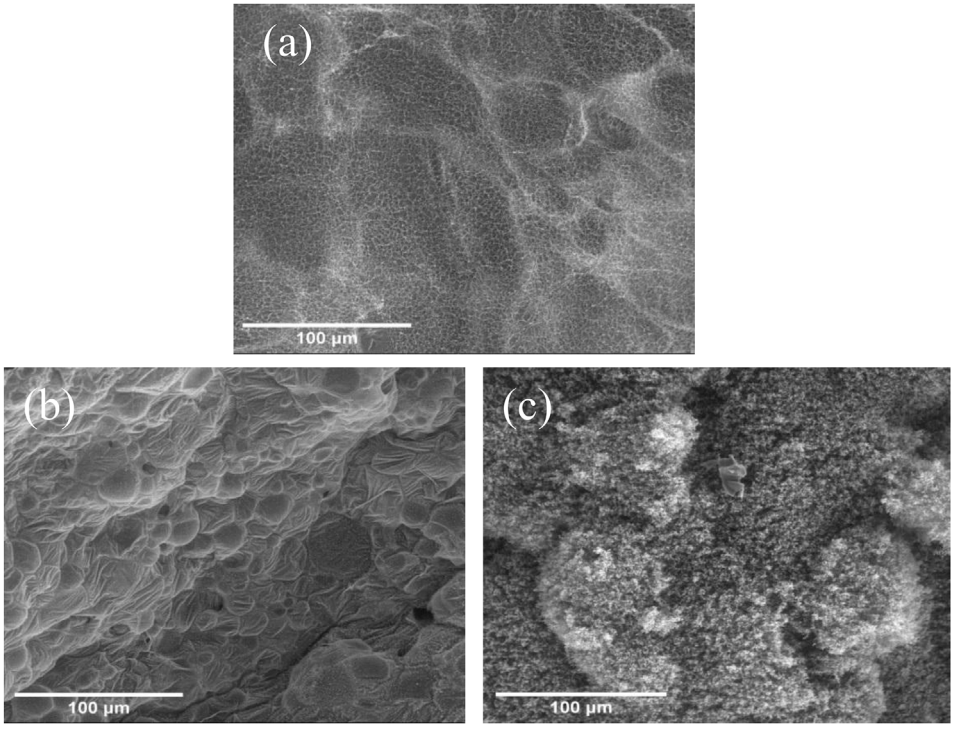

Fig. 6. SEM images of char surface for (a) EP20A, (b) EP18A2HNT and (c) EP18A2LDH samples after cone calorimeter testing.

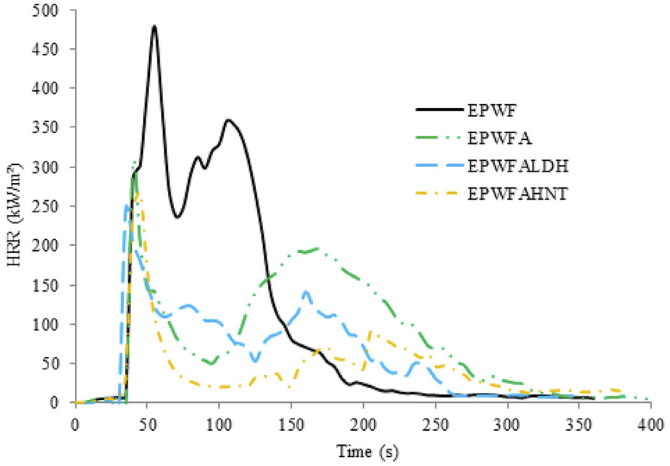

Fig. 7. Heat release rate curves as a function of time for fibre reinforced epoxy composites at 50 kW/m^2 heat flux.

UL-94 and LOI results indicated that the self-extinguishing behaviour of the fibre reinforced composites was considerably enhanced in the presence of the additives.

3.3.3. Flame retardant mechanisms

The authors have proposed that the fire reaction properties of the epoxy blend containing LDH were enhanced due to the migration of LDH particles to the surface of the sample, forming a protective ceramic-like char. As the temperature increased under the cone heater, the decomposition of polymer and formation of volatile products gradually led to a pressure build-up inside the sample. The rising bubbles of the decomposition products pushed the LDH particles toward the surface of the blend. At higher temperatures, the LDH particles started to decompose to metal oxide, H_2O and CO_2. The metal oxide residues covered the surface of the sample and acted as a physical barrier against heat and fire to protect the under-lying polymer from further decomposition. In the meantime, the released H_2O and CO_2 helped the formed char to expand and swell [3,48]. In the case of the blends containing both APP and nano-particles, the decomposition of APP and intumescent char formation was the main flame retardant mechanism. Furthermore, the LDH and HNT particles could enhance the formed intumescent char in two different ways. Fig. 8(a) and (b) present schematic illustrations of the intumescent char formation process for the epoxy blends containing APP/LDH and APP/HNT, respectively. The aforementioned charring effect of LDH provided an additional barrier for the intumescent char, further improving its insulating properties. The released H_2O and CO_2 gases from the LDH could also enhance the intumescent behaviour of the char and dilute the oxygen concentration above the sample. However, the HNT particles physically reinforced the intumescent char by providing an aluminosilicate skeleton frame, as has been reported previously [33]. The nano-tubes with large aspect ratio could bridge and make a network to enhance the stability of the intumescent char at high temperatures.

Table 3
Cone calorimeter data and results of UL-94 and LOI tests for fibre reinforced epoxy composites.

Sample	Time to ignition (s)	Peak heat release rate (kW/m^2)	Total heat release (MJ/m^2)	UL-94 Rating	Limiting oxygen index (%)
EPWF	21 ± 2	453.5 ± 36	36.2 ± 0.8	No Rating	22.1 ± 0.2
EPWFA	20 ± 2	290.4 ± 17.2	32.2 ± 2.1	V-1	32 ± 0.3
EPWFALDH	21 ± 1	258.7 ± 17.7	22.6 ± 2.1	V-1	31.7 ± 0.2
EPWFAHNT	22 ± 2	262 ± 8.4	18.4 ± 5	V-1	31.4 ± 0.3

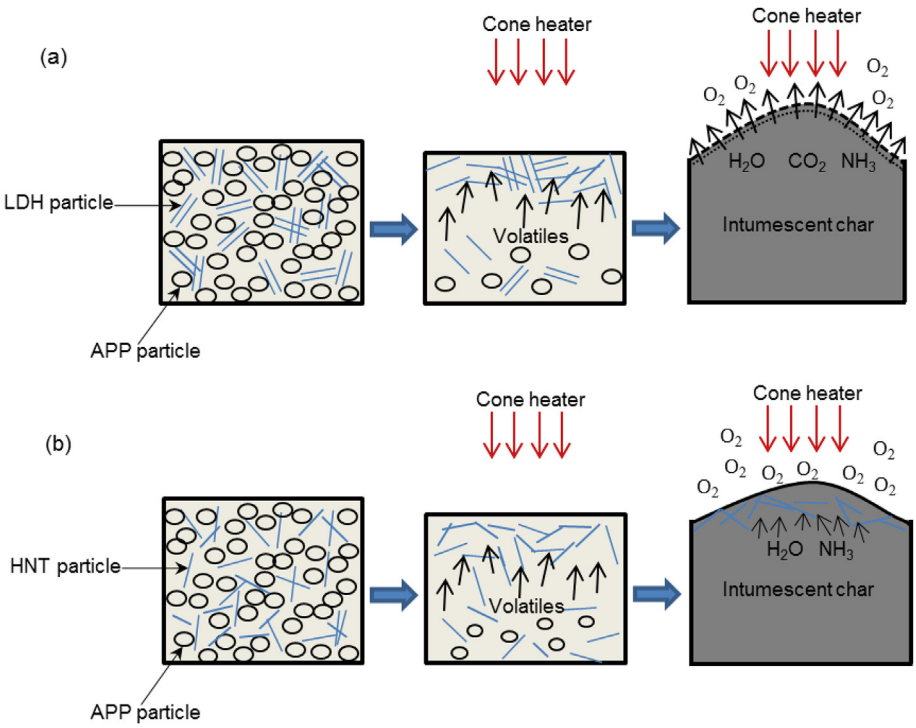

Fig. 8. Schematic illustrations of intumescent char formation process in (a) APP/LDH and (b) APP/HNT epoxy blends..

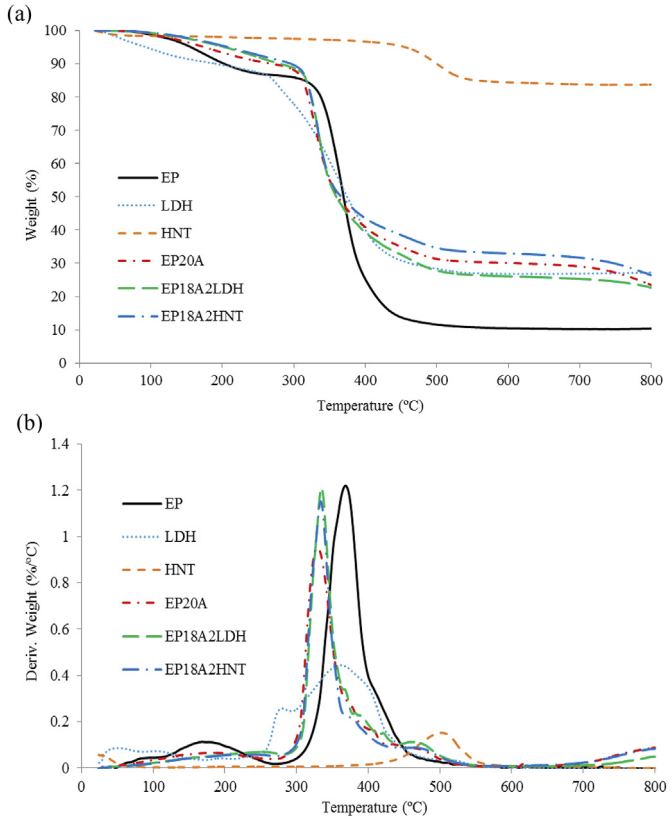

Fig. 9. (a) TG and (b) DTG curves of pure epoxy, nano-particles and blends in nitrogen atmosphere.

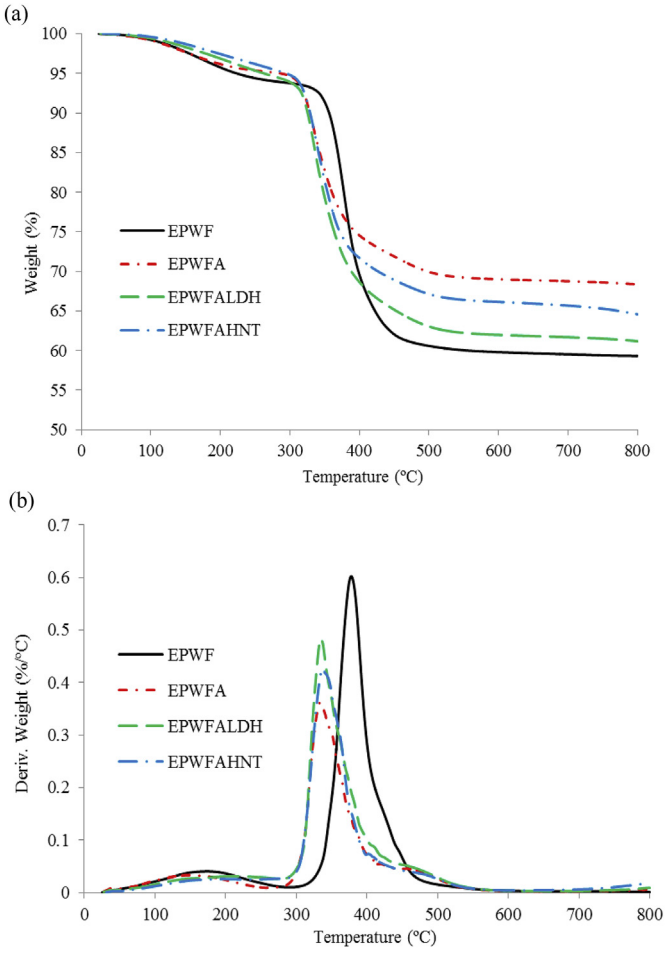

Fig. 10. (a) TG and (b) DTG curves of fibre reinforced epoxy composites in nitrogen atmosphere.

Table 4
Tensile, flexural and compression properties of epoxy resin, blends and composites.

Sample	Tensile Strength (MPa)	Flexural Strength (MPa)	Tensile Modulus (GPa)	Flexural Modulus (GPa)	Compression Strength (MPa)
EP	58.8 ± 1.2	102 ± 4.4	3.05 ± 0.06	3.43 ± 0.15	–
EP18A2LDH	41.1 ± 0.9	73.3 ± 2.3	3.60 ± 0.25	3.63 ± 0.07	–
EP18A2HNT	39.5 ± 1.1	73.7 ± 3.3	3.60 ± 0.10	3.61 ± 0.14	–
EP20A	41.3 ± 1.2	70.9 ± 2.0	4.07 ± 0.24	3.83 ± 0.13	–
EPWF	399.5 ± 14.8	401.6 ± 14.2	18.8 ± 0.9	14.7 ± 0.4	284.2 ± 23.9
EPWFALDH	342.4 ± 4.8	397 ± 2.4	16.2 ± 0.6	14.7 ± 0.1	273.7 ± 9.7
EPWFAHNT	394.7 ± 12.0	438.2 ± 11.5	17.9 ± 0.6	15.3 ± 0.3	278 ± 7.3
EPWFA	385.2 ± 10.2	418.4 ± 13.3	17.9 ± 0.3	15.1 ± 0.3	291.6 ± 6.9

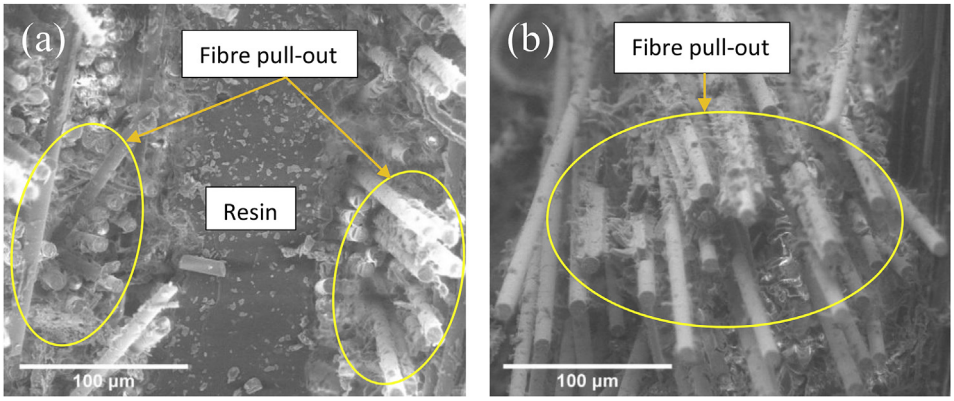

Fig. 11. SEM images of tensile fractured cross-sections: (a) EPWF and (b) EPWFALDH samples.

3.4. TGA

Fig. 9(a) and (b) demonstrate the thermogravimetric (TG) and derivative thermogravimetric (DTG) curves, respectively, of pure epoxy resin, the nano-particles and blends in a nitrogen atmosphere. The TG curves in Fig. 9 show that the main decomposition step of epoxy resin occurs at the temperature range of 300–450 °C due to the chain scission and fragmentation of epoxy. Furthermore, the main decomposition of LDH (~60% weight loss) takes place approximately between 250 and 500 °C as the result of de-hydroxylation and decomposition of organic species [6] but HNT is relatively stable up to 800 °C and shows only around 13% weight reduction at the temperature range of 400–550 °C because of de-hydroxylation. Regarding the thermal decomposition of blends, the epoxy blends containing APP start to decompose earlier than the neat epoxy due to the lower decomposition temperature of APP compared to that of the resin matrix. However, the blends show higher amounts of residue over approximately 370 °C due to the formation of protective intumescent char during thermal decomposition. In addition, the partial substitution of APP with LDH leads to the higher weight reduction of the blend above 370 °C compared to that of the sample containing only APP. This behaviour could be correlated to the thermal degradation of the LDH nano-particles and the release of H_2O and CO_2 gases, which would accelerate the decomposition of the blend. However, the relatively high thermal stability of HNT particles served to improve the thermal insulation of the char and increase the residue mass from the sample (EP18A2HNT) at high temperatures.

The TG and DTG curves of the fibre reinforced composites are illustrated in Fig. 10(a) and (b), respectively. It can be seen that the onset decomposition temperature of epoxy/glass fibre composite decreases but its thermal stability increases at high temperatures (over approximately 370 °C) in the presence of APP (similar to the behaviour of epoxy blends). In addition, the composite containing APP and HNT unexpectedly exhibited higher weight reduction (lower thermal stability) at high temperatures compared to that of the composite filled only with APP. This lower thermal stability can be attributed to the trapping of HNT particles between the glass fibre plies, which hinders the thermal insulating effect of the particles on the formed char compared to the samples without fibres. In general, the composite samples generated higher volume of residue in the presence of the glass fibres at the end of the tests, since glass fibres are completely stable at this temperature range.

3.5. Mechanical properties

Table 4 summarises the tensile, flexural and compression properties of the epoxy resin, its blends and composites. The incorporation of APP and nano-particles reduced the mechanical strengths of epoxy resin but slightly improved the mechanical moduli of the resin. The reduction in the mechanical strengths can be attributed to the incompatibility of the APP particles with the polymer matrix [46,49]. On the other hand, the possible reduction of the inter-particles distances by the application of additives can improve the deformation resistance and moduli of the samples [50]. Furthermore, there are not significant differences between the mechanical properties of the EP18A2LDH and EP18A2HNT and those of the EP20A, since APP is the main additive and possibly hinders the reinforcing effects of the nano-particles. Moreover, as expected, the addition of glass fibre reinforcement significantly improved the mechanical properties of the composites. The fibre reinforced composites containing additives showed similar tensile, flexural and compression properties compared to those of reference composite without any additives. However, the tensile properties of the epoxy/glass fibre composite slightly decreased by incorporation of APP and LDH. This reduction can be correlated to the increased viscosity of the resin in the presence of the two dimensional LDH nano-particles and consequently decreased interfacial bonding between the resin and fibres. Fig. 11(a) and (b) present scanning micrographs of the fractured cross-sections of the EPWF and EPWFALDH composites, respectively, produced under tensile loading. It is clearly seen that the fractured surface of the EPWFALDH sample shows more fibre pull-out compared to that of the EPWF composite and this indicates the lower interfacial bonding between the resin and fibre when APP and LDH are incorporated. Overall, the results demonstrate that the reinforcing fibres

play the dominant role to determine the mechanical properties of fibre composites.

4. Conclusions

This research focussed on comparing the fire and mechanical properties of epoxy blends and composites containing LDH and HNT. The results showed that the fire performance of the epoxy nano-clay blends was insufficient to achieve any vertical burn rating and enhance the LOI value. However, as expected, the incorporation of APP and nano-particles significantly enhanced the flame retardancy and thermal stability of the epoxy resin and epoxy/glass fibre systems. The tensile and flexural strengths of the resin reduced in the presence of additives, while both moduli slightly improved. Insignificant changes were observed in the mechanical properties of fibre reinforced composites with the incorporation of the additives (APP and nano-particles). When APP was added, the epoxy composites containing APP/HNT and APP/LDH demonstrated similar trends of fire properties in the cone calorimeter, vertical burn and LOI tests. The samples including HNT, however, showed lower THR values compared to those of the samples containing LDH. The tensile properties of the glass fibre epoxy composite filled with APP/HNT were also slightly higher than those of the composite containing APP/LDH. By considering the lower price of HNT (~1.5 USD/kg) in comparison to those of LDH (~180 USD/kg) and APP (13–14 USD/kg), we note that the application of HNT can be more effective for the design of flame retardant and mechanically sound composites. Reducing the materials cost can also be beneficial for the mass productions and industrial applications of the composites.

Acknowledgments

The authors gratefully acknowledge Ministry for Business, Innovation and Employment, New Zealand for financial support (grant number: UOAX1415). The technical support of CACM technicians for this research is also acknowledged.

References

[1] Bar M, Alagirusamy R, Das A. Flame retardant polymer composites. Fibers Polym 2015;16(4):705–17.
[2] Mngomezulu ME, John MJ, Jacobs V, Luyt AS. Review on flammability of biofibres and biocomposites. Carbohydr Polym 2014;111:149–82.
[3] Jiang DD. 11 Polymer nanocomposites. In: Wilkie CA, Morgan AB, editors. Fire retardancy of polymeric materials. New York: Taylor & Francis; 2009. p. 261–99.
[4] Gao Y, Wu J, Wang Q, Wilkie CA, O'Hare D. Flame retardant polymer/layered double hydroxide nanocomposites. J Mater Chem 2014;2(29):10996–1016.
[5] Manzi-Nshuti C, Songtipya P, Manias E, Jimenez-Gasco MM, Hossenlopp JM, Wilkie CA. Polymer nanocomposites using zinc aluminum and magnesium aluminum oleate layered double hydroxides: effects of LDH divalent metals on dispersion, thermal, mechanical and fire performance in various polymers. Polymer 2009;50(15):3564–74.
[6] Nyambo C, Chen D, Su S, Wilkie CA. Does organic modification of layered double hydroxides improve the fire performance of PMMA? Polym Degrad Stabil 2009;94(8):1298–306.
[7] Wang L, Su S, Chen D, Wilkie CA. Variation of anions in layered double hydroxides: effects on dispersion and fire properties. Polym Degrad Stabil 2009;94(5):770–81.
[8] Mishra G, Dash B, Pandey S. Layered double hydroxides: a brief review from fundamentals to application as evolving biomaterials. Appl Clay Sci 2018;153:172–86.
[9] Li Z, Liu L, González AJ, Wang D-Y. Bioinspired polydopamine-induced assembly of ultrafine Fe $(OH)_3$ nanoparticles on halloysite toward highly efficient fire retardancy of epoxy resin via an action of interfacial catalysis. Polym Chem 2017;8(26):3926–36.
[10] Zhang Y, Tang A, Yang H, Ouyang J. Applications and interfaces of halloysite nanocomposites. Appl Clay Sci 2016;119:8–17.
[11] Krishnaiah P, Ratnam CT, Manickam S. Development of silane grafted halloysite nanotube reinforced polylactide nanocomposites for the enhancement of mechanical, thermal and dynamic-mechanical properties. Appl Clay Sci 2017;135:583–95.
[12] Beyer G, Lan T. Polymer nanocomposites: a nearly universal FR synergist. In: Wilkie CA, Morgan AB, editors. Non-halogenated flame retardant handbook. Wiley; 2014. p. 243–92.
[13] Liu M, Jia Z, Jia D, Zhou C. Recent advance in research on halloysite nanotubes-polymer nanocomposite. Prog Polym Sci 2014;39(8):1498–525.
[14] George G, Selvakumar M, Mahendran A, Anandhan S. Structure–property relationship of halloysite nanotubes/ethylene–vinyl acetate–carbon monoxide terpolymer nanocomposites. J Thermoplast Compos Mater 2017;30(1):121–40.
[15] Matusinovic Z, Wilkie CA. Fire retardancy and morphology of layered double hydroxide nanocomposites: a review. J Mater Chem 2012;22(36):18701–4.
[16] Liu TX, Zhu H. Flame retardant properties of polymer/layered double hydroxide N nanocomposites. In: Pandey JK, Reddy KR, Mohanty AK, Misra M, editors. Handbook of polymer nanocomposites processing, performance and application. New York: Springer; 2014. p. 389–414.
[17] Kausar A. Review on polymer/halloysite nanotube nanocomposite. Polym Plast Technol Eng 2018;57(6):548–64.
[18] Edenharter A, Feicht P, Diar-Bakerly B, Beyer G, Breu J. Superior flame retardant by combining high aspect ratio layered double hydroxide and graphene oxide. Polymer 2016;91:41–9.
[19] Kiliaris P, Papaspyrides C. Polymer/layered silicate (clay) nanocomposites: an overview of flame retardancy. Prog Polym Sci 2010;35(7):902–58.
[20] Laoutid F, Bonnaud L, Alexandre M, Lopez-Cuesta J-M, Dubois P. New prospects in flame retardant polymer materials: from fundamentals to nanocomposites. Mater Sci Eng R 2009;63(3):100–25.
[21] Liu S, Fang Z, Yan H, Chevali VS, Wang H. Synergistic flame retardancy effect of graphene nanosheets and traditional retardants on epoxy resin. Composites Part A 2016;89:26–32.
[22] Sun J, Gu X, Coquelle M, Bourbigot S, Duquesne S, Casetta M, et al. Effects of melamine polyphosphate and halloysite nanotubes on the flammability and thermal behavior of polyamide 6. Polym Adv Technol 2014;25(12):1552–9.
[23] Dewaghe C, Lew C, Claes M, Dubois P. Fire-retardant applications of polymer–carbon nanotubes composites: improved barrier effect and synergism. In: McNally T, Potschke P, editors. Polymer–carbon nanotube composites. Elsevier; 2011. p. 718–45.
[24] Bourbigot S, Duquesne S, Fontaine G, Bellayer S, Turf T, Samyn F. Characterization and reaction to fire of polymer nanocomposites with and without conventional flame retardants. Molecular Cryst liq Cryst 2008;486(1). 325/[1367]-339/[1381].
[25] Du B, Guo Z, Song Pa, Liu H, Fang Z, Wu Y. Flame retardant mechanism of organo-bentonite in polypropylene. Appl Clay Sci 2009;45(3):178–84.
[26] Ma H, Tong L, Xu Z, Fang Z. Intumescent flame retardant-montmorillonite synergism in ABS nanocomposites. Appl Clay Sci 2008;42(1–2):238–45.
[27] Zhong Y, Wu W, Lin X, Li M. Flame-retarding mechanism of organically modified montmorillonite and phosphorous-nitrogen flame retardants for the preparation of a halogen-free, flame-retarding thermoplastic poly (ester ether) elastomer. J Appl Polym Sci 2014;131(22):1–9.
[28] Chen Y, Fang Z, Yang C, Wang Y, Guo Z, Zhang Y. Effect of clay dispersion on the synergism between clay and intumescent flame retardants in polystyrene. J Appl Polym Sci 2010;115(2):777–83.
[29] Zhao C-X, Liu Y, Wang D-Y, Wang D-L, Wang Y-Z. Synergistic effect of ammonium polyphosphate and layered double hydroxide on flame retardant properties of poly (vinyl alcohol). Polym Degrad Stabil 2008;93(7):1323–31.
[30] Tang Y, Hu Y, Wang S, Gui Z, Chen Z, Fan W. Intumescent flame retardant–montmorillonite synergism in polypropylene-layered silicate nanocomposites. Polym Int 2003;52(8):1396–400.
[31] Liu YJ, Mao L, Fan Sh. Preparation and study of intumescent flame retardant poly (butylene succinate) using MgAlZnFe-CO_3 layered double hydroxide as a synergistic agent. J Appl Polym Sci 2014;131(17):1–10.
[32] Li Z, Shah AR, Prabhakar M, Song J-i. Effect of inorganic fillers and ammonium polyphosphate on the flammability, thermal stability, and mechanical properties of abaca-fabric/vinyl ester composites. Fibers Polym 2017;18(3):555–62.
[33] Lecouvet B, Sclavons M, Bailly C, Bourbigot S. A comprehensive study of the synergistic flame retardant mechanisms of halloysite in intumescent polypropylene. Polym Degrad Stabil 2013;98(11):2268–81.
[34] Deng S, Zhang J, Ye L. Halloysite–epoxy nanocomposites with improved particle dispersion through ball mill homogenisation and chemical treatments. Compos Sci Technol 2009;69(14):2497–505.
[35] Luo P, Zhang J-s, Zhang B, Wang J-h, Zhao Y-f, Liu J-d. Preparation and characterization of silane coupling agent modified halloysite for Cr (VI) removal. Ind Eng Chem Res 2011;50(17):10246–52.
[36] Mahboobeh E, Yunus WMZW, Hussein Z, Ahmad M, Ibrahim NA. Flexibility improvement of poly (lactic acid) by stearate-modified layered double hydroxide. J Appl Polym Sci 2010;118(2):1077–83.
[37] Du M, Guo B, Jia D. Thermal stability and flame retardant effects of halloysite nanotubes on poly (propylene). Eur Polym J 2006;42(6):1362–9.
[38] Marney D, Russell L, Wu D, Nguyen T, Cramm D, Rigopoulos N, et al. The suitability of halloysite nanotubes as a fire retardant for nylon 6. Polym Degrad Stabil 2008;93(10):1971–8.
[39] Wang X, Rathore R, Songtipya P, del Mar Jimenez-Gasco M, Manias E, Wilkie CA. EVA-layered double hydroxide (nano) composites: mechanism of fire retardancy. Polym Degrad Stabil 2011;96(3):301–13.
[40] Costache MC, Heidecker MJ, Manias E, Camino G, Frache A, Beyer G, et al. The influence of carbon nanotubes, organically modified montmorillonites and layered double hydroxides on the thermal degradation and fire retardancy of polyethylene, ethylene–vinyl acetate copolymer and polystyrene. Polymer 2007;48(22):6532–45.
[41] Costa FR, Wagenknecht U, Heinrich G. LDPE/Mg–Al layered double hydroxide nanocomposite: thermal and flammability properties. Polym Degrad Stabil 2007;92(10):1813–23.
[42] Schartel B, Bartholmai M, Knoll U. Some comments on the main fire retardancy mechanisms in polymer nanocomposites. Polym Adv Technol 2006;17(9–10):772–7.
[43] Rajaei M, Kim NK, Bhattacharyya D. Effects of heat-induced damage on impact performance of epoxy laminates with glass and flax fibres. Compos Struct 2018;185:515–23.

[44] Kim NK, Dutta S, Bhattacharyya D. A review of fire properties of natural fibre reinforced polymeric composites. Compos Sci Technol 2018;162:64–78.
[45] Kim NK, Lin R, Bhattacharyya D. Flammability and mechanical behaviour of polypropylene composites filled with cellulose and protein based fibres: a comparative study. Composites Part A 2017;100:215–26.
[46] Rajaei M, Wang D-Y, Bhattacharyya D. Combined effects of ammonium polyphosphate and talc on the fire and mechanical properties of epoxy/glass fabric composites. Composites Part B 2017;113:381–90.
[47] Chai M, Bickerton S, Bhattacharyya D, Das R. Influence of natural fibre reinforcements on the flammability of bio-derived composite materials. Composites Part B 2012;43(7):2867–74.
[48] Zammarano M, Franceschi M, Bellayer S, Gilman JW, Meriani S. Preparation and flame resistance properties of revolutionary self-extinguishing epoxy nanocomposites based on layered double hydroxides. Polymer 2005;46(22):9314–28.
[49] Kim NK, Bhattacharyya D. Development of fire resistant wool polymer composites: mechanical performance and fire simulation with design perspectives. Mater Des 2016;106:391–403.
[50] Neitzel I, Mochalin V, Knoke I, Palmese GR, Gogotsi Y. Mechanical properties of epoxy composites with high contents of nanodiamond. Compos Sci Technol 2011;71(5):710–6.